Understanding multi-stage HCCI combustion caused by thermal stratification and chemical three-stage auto-ignition

Moez Ben Houidi*[a], Abdullah AlRamadan [a], Julien Sotton[b], Marc Bellenoue[b], S. Mani Sarathy [a], Bengt Johansson[a]

[a] *King Abdullah University of Science and Technology (KAUST), CCRC, PSE, Thuwal 23955-6900, Saudi Arabia.*

[b] *ISAE-ENSMA, Institut PPRIME, departement Fluide Thermique Combustion, BP 40109, Teleport2, 1 avenue Clement Ader, F86961 Futuroscope Chasseneuil-du-Poitou Cedex, France.*

*corresponding author. E-mail address: moez.benhouidi@kaust.edu.sa

Keywords: *RCM, three-stage auto-ignition, n-heptane, n-hexane, HCCI.*

Abstract

The Homogeneous Charge Compression Ignition (HCCI) concept shows great potential for improving engine efficiency and reducing pollutant emissions. However, the operation with this concept in Internal Combustion (IC) engines is still limited to low speed and load conditions, as excessive Pressure Rise Rates (PRR) are generated with its fast auto-ignition. To overcome this limitation, the use of moderate thermal and charge stratification has been promoted. This leads to multi-stage ignition, and thus a potentially acceptable PRR. Recently [1], three-stage auto-ignition has been emphasized as a chemical phenomenon where the thermal runaway is inhibited during the main ignition event. The current paper demonstrates experimental evidence on this phenomenon observed during n-heptane and n-hexane auto-ignition at lean diluted conditions in a flat piston Rapid Compression Machine (RCM). Multi-stage ignition events caused by either chemical kinetics or by the well-known thermal stratification of this type of RCM are clearly identified and differentiated. The combination of these two factors seems to be a suitable solution to overcome PRR limitations.

1. Introduction

The homogeneous charge compression ignition (HCCI) concept has been extensively studied [2-4], as it is a potential technology to improve efficiency and to reduce emissions of internal combustion (IC) engines. Engine operation with this mode has been limited to relatively low loads for two major reasons: (i) the control of the combustion timing, which is mainly dependent on the fuel/air mixture reactivity [5, 6] and (ii) the excessive pressure rise rate (PRR), which increases too much the noise level and the knock intensity [7]. In addition to

reactivity controlled compression ignition (RCCI) [8], the use of charge stratification has been one of the major solutions proposed to overcome these limitations [9, 10]. All these technologies aim at generating multi-zone auto-ignitions and thereby control the overall combustion phasing.

The stratification of the charge, with temperature and composition heterogeneities, is different from the chemically driven multi-stage auto-ignition. The latter is typically associated in the literature with two-stage heat release (HR), a feature of alkane auto-ignition [5, 11]. The ignition initiates by a low-temperature heat release (LTHR) stage driven by the decomposition of highly oxygenated intermediates [12]. The negative temperature coefficient (NTC) chemistry, identified by the production of olefins and HO_2 radicals from RO_2, inhibits the low-temperature chemistry from proceeding to thermal runaway [12]. After that, the main ignition event occurs with higher absolute heat addition. The production of OH radicals from H_2O_2 decomposition, radical chain branching from $H+O_2$, and oxidation of CO to CO_2 are the main contributors to high-temperature heat release (HTHR). Some studies have reported an auto-ignition phenomenon with an additional third HR stage described as intermediate temperature heat release (ITHR) [13-15] or delayed HTHR [16, 17]. These studies either attribute the added HTHR stage to thermal stratifications, inhibition of reactivity due to radicals for dual fuel mixtures, or transport phenomenon. Sarathy et al. [1] recently reported a purely chemically-driven three-stage auto-ignition observed with lean n-heptane mixtures at low temperatures. In [1], the HTHR is divided into two stages where reactivity is suppressed by H, OH, and HO_2 radical termination pathways. It is worth highlighting that the ITHR reported in [14, 15, 18] and the three-stage HR reported in [1] are two different phenomena. The ITHR occurs between the first stage (LTHR) and second stage (HTHR), where the temperature corresponding to it is in the range of 850 K to 950 K depending on the conditions. However, the three-stage HR is rather a splitting of the HTHR, where the second stage occurs at a temperature higher than 1150 K. Indeed, this difference in temperature at which these phenomena exists points to distinct chemical kinetic phenomenon governing each. The ITHR is governed by low and intermediate radical chain branching/termination reactions involving QOOH radicals. However, the three-stage HR observed in [1] is governed by HO2 and OH radical recombination reactions at high temperature. To the authors' knowledge, no studies have been reported previously on how chemically driven multi-stage HR is clearly differentiated from the multi-stage ignition caused by charge stratification.

This paper focuses on investigating chemically driven multi-stage HR in a flat piston RCM, where thermal stratification has been previously demonstrated and characterized [19-21]. RCMs have been widely used for the study of fuel's chemical kinetics [22, 23]. It is well known that the use of a flat piston generates significantly higher temperature stratification inside the RCM chamber, which affects ignition delay measurements [21, 24-26]. This

has motivated the use of piston crevice, which has greatly simplified the development and validation of detailed chemical mechanisms [22, 23]. Nevertheless, the crevice volume has to be optimized to effectively suppress the temperature heterogeneity generated by the roll-up vortices in a wide range of test conditions [27-29]. Besides, a substantial mass flow to the crevice during the combustion may significantly influence the measured ignition delays [30]. This motivated to use the crevice containment concept [31-33], which may further facilitate the validation of chemical kinetic simulations.

In the following, the experimental setup and simulation methods will be first presented. The experimental results report pressure and chemiluminescence intensity profiles. The simulation results show the concentration profiles of the main species involved in chemically driven two-stage and three-stage auto-ignition.

2. Methodology

2.1 Flat piston RCM

Experiments are performed in the RCM of PPRIME Institute in Poitiers. A schematic of this device is presented in Figure 1. The operation of this facility is detailed in previous studies [21, 34-36]. The RCM has a particular square section chamber and optical access through flat sapphire or quartz windows. This has the advantage of allowing optical diagnostics without the need for image distortion correction. In the current work, the RCM is operated at a compression ratio of 9, which corresponds to a chamber volume of 132 cm^3 at the top dead center (TDC). A lateral cross-section view of the RCM combustion chamber is illustrated in Figure 2. The in-cylinder pressure is acquired at 100 kHz with a piezoelectric transducer coupled to a charge amplifier where no-hardware filtering was used. The pressure signal is converted to absolute pressure then filtered using a low pass finite impulse response (FIR) filter set to a threshold of 5 kHz. For later analysis, the PRR is defined as the time-derivative of the filtered pressure dP/dt, which is also filtered using the same low pass FIR filter with a threshold of 3 kHz. As the RCM chamber is kept at a constant volume after the end of compression (EOC), the heat release rate (HRR) can be modeled as follows:

$$HRR = \frac{dQ}{dt} = \frac{1}{\gamma - 1} V \frac{dP}{dt} + \frac{dQ_{ht}}{dt} \quad (1)$$

Where γ is the heat capacity ratio, V is the volume, and Q_{ht} is the heat loss. As demonstrated in [37, 38], the heat transfer is negligible compared to the heat of combustion, and the HRR is expected to be highly proportional to the PRR. Thus, the peaks of the HRR can be easily detected by identifying the peaks of the PRR. In the following, the PRR will be used to identify the type of multi-stage ignition. This parameter has also the benefit of indicating the noise propensity of the combustion, which is considered as one of the main limitations to operate IC engines at HCCI mode.

The current work is focused on the auto-ignition of lean diluted n-heptane and n-hexane reactive mixtures at low to intermediate temperatures. The test conditions are detailed in Table 1, where also the measured ignition delay times (IDT) are reported. In all studied cases, the equivalence ratio and O_2 concentration have been fixed, respectively, at 0.4 and 16.1 %mol. All tests are repeated at least three times to check the consistency of results. In Table 1, τ_1, τ_2, and τ_3 correspond respectively to the IDT of the first, second, and third stage. These delays are defined as the time gaps between the EOC and the peak of PRR corresponding to each stage. During these tests, a CMOS fast camera is focused on the central plane of the RCM chamber to record chemiluminescence at a frame rate of, respectively, 28 kHz and 42 kHz for n-heptane and n-hexane cases. A Sigma lens with a focal length of 105 mm at 2.8 is used, which allows a field depth of approximately 40% the size of the combustion chamber. No selective filters have been used in the current configuration.

The internal aerodynamics of the flat piston RCM in PPRIME institute has been extensively studied [19, 20]. The previous characterization has demonstrated how the roll-up vortices, generated by the piston motion, mix the cold boundary layer with the adiabatically compressed gases. Two-dimensional temperature fields from planar laser-induced fluorescence (PLIF), performed at test conditions similar to the current study, have been reported in [21]. This analysis identified the location of these two distinctive zones during the post-compression period. In [21], it has been demonstrated that up to 48 ms after TDC, the adiabatically compressed gases are located in the upper areas of the chamber, while the colder gases entrained by the roll-up vortices are still in the bottom and central sides of the chamber. In [39], additional investigation using thin-wire thermometry has demonstrated that the adiabatic core hypothesis is valid up to approximately 70 ms after TDC (at the same test conditions). This characterization allowed studying the thermo-kinetic interactions caused by these temperature heterogeneities.

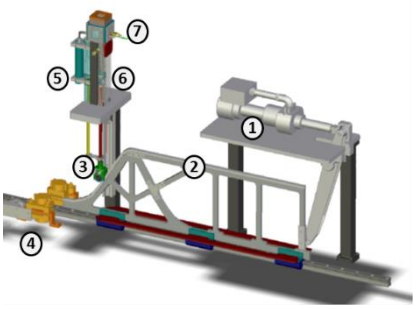

Figure 1. Schematic of the PPRIME institute RCM: (1) Hydraulic cylinder, (2) Cam, (3) Guiding wheel, (4) Brake system, (5) Return pneumatic cylinder, (6) Piston/cylinder, (7) Combustion chamber.

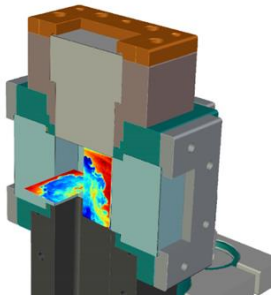

Figure 2. Illustration of the cubic shape combustion chamber of the RCM.

Table 1. Summary of experimental test conditions and results. Φ, P_c, and T_c are respectively the equivalence ratio, the pressure, and the adiabatic core temperature at TDC.

Fuel	**Composition** (Fuel/ O_2 / N_2 / Ar %mol)	**Φ** **(-)**	**ρ** (kg/m^3)	**P_c** (bar)	**T_c** (K)	**τ_1** (ms)	**τ_2** (ms)	**τ_3** (ms)
n-heptane	0.59/16.1/59.65/23.66	0.4	9.3	15.7	699	1 ± 0.1	6.2 ± 0.2	7.1 ± 0.3
n-hexane	0.68/16.09/59.64/23.59	0.4	9.1	15.7	703	1.8 ± 0.1	6.8 ± 0.2	7.5 ± 0.2
n-hexane	0.68/16.09/27.81/55.42	0.4	9.1	15.6	791	-3.4 ± 0.1	0.8 ± 0.2	-

2.2 Chemical kinetic modeling

Detailed chemical kinetic simulations were performed for all the test conditions of Table 1. The updated n-heptane kinetic model of Zhang et al. [40], composed of 1268 species and 5336 reactions, is implemented in CHEMKIN PRO and used for the simulation with the homogenous batch reactor model. The same kinetic model was used to simulate both n-heptane and n-hexane mixtures. Effective volume profiles were considered for the simulations [22]. This effective volume is deduced from the compression of an inert gas mixture performed at similar test conditions. The adiabatic core temperature profile of the inert run is calculated using the following equation:

$$\int_{T_0}^{Tc} \frac{\gamma}{\gamma - 1} \frac{dT}{T} = \ln\left(\frac{P_c}{P_0}\right) \qquad (2)$$

Where T_0 and P_0 are, respectively, the initial temperature and pressure. The volume is then deduced based on the ideal gas assumption. At the EOC, the effective volume is larger than the geometrical one and increases progressively in the post-compression period. With this simplified method, the heat losses of the RCM are partly considered in the simulation. It was checked that the temperature and pressure profiles of experiments and simulations are in excellent agreement. The PRR is also calculated from the pressure profile of simulation. It is worth noting that the simulated PRR was filtered similarly to the experimental case.

3. Results

3.1 Evidence of three-stage auto-ignition

The auto-ignition behavior of n-heptane at a T_c of 699 K is detailed in Figure 3. This schematic shows a sequence of chemiluminescence images recorded during the HTHR period. At the upper side of these images, the pressure profiles are reported with an indication (by a solid red line) of the instant at which the image was recorded. On the bottom of the images, the intensity profiles in the central line (location identified with a dashed line) are reported. The PRR clearly shows a staged auto-ignition where three steps are easily identified by tracking the local maxima. The first peak corresponds to LTHR, while the second and third correspond to HTHR. Figure 3 demonstrates that the chemiluminescence signal is not detected, up to the start of the second stage ignition. A weak chemiluminescence intensity is then observed in the upper area of the RCM chamber at the second stage (t = 6.2 ms). The intensity significantly increases with the onset of the third stage ignition in the same location inside the chamber. The auto-ignition in the bottom part, which corresponds to the auto-ignition of the colder gases in the roll-up vortices, is observed after the third stage ignition. As demonstrated in [21, 39], the combustion propagation in the current case is mainly dominated by the reaction front propagation regime [41], also called 'spontaneous ignition front' in the literature. Figure 3 demonstrates that the sequential auto-ignition imposed by thermal stratification inside the RCM chamber is not correlated to the three-stage observed on the PRR. Thus, the staged PRR is a chemically driven phenomenon.

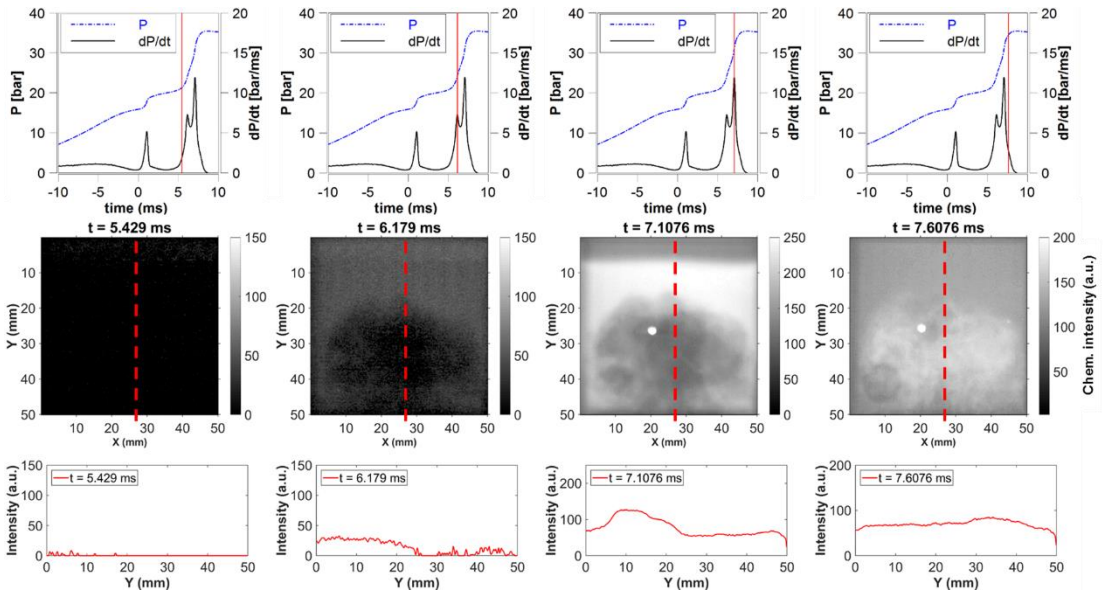

Figure 3. Comparison of pressure traces and chemiluminescence during a three-stage auto-ignition of n-heptane lean diluted mixture (T_c = 699 K).

To corroborate the above result for n-heptane, the same test condition has been reproduced with n-hexane. The analysis, reported in Figure 4, is focused on the main ignition. The auto-ignition of a lean diluted n-hexane mixture at a T_c of 703 K also demonstrates a similar three-stage PRR. In Figure 4, the chemiluminescence images are

compared to the PRR during the HTHR, while the local intensity profiles are reported in the same graph. The local chemiluminescence is averaged on a 3x3 mm^2 area, in the upper side (referred to as "Chem. 1") and in the bottom side (referred to as "Chem. 2"). It is demonstrated that the local chemiluminescence profile, corresponding to the auto-ignition of the adiabatically compressed gases, has an intensity peak synchronized with the third-stage ignition. The local chemiluminescence profile at the bottom of the chamber has its peak after the third ignition and does not induce a fourth peak in the PRR. This fact also proves that this phenomenon is different from the sequential auto-ignition that has been investigated in [21, 39].

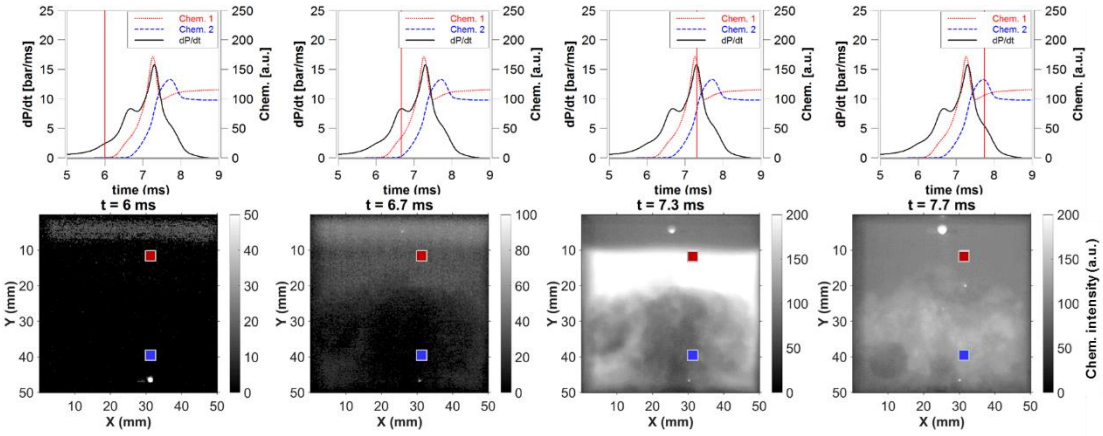

Figure 4. Illustration of the multi-stage auto-ignition of a lean diluted n-hexane mixture (T_c = 703 K).

When increasing the compression temperature of the lean diluted n-hexane mixture up to 791 K, the auto-ignition has only a two-stage PRR as demonstrated in Figure 5. In Figure 6, the multi-stage auto-ignition of this higher temperature case is illustrated similarly to the previous case of Figure 5. Here, the HTHR stage shows only a single stage, and the peak PRR is synchronized with the peak of the local chemiluminescence intensity in the upper side of the chamber. The intensity profiles have a sharper increase compared to the lower temperature case of Figure 4. All of the aforementioned experimental facts demonstrate that the three-stage auto-ignitions observed at lean diluted conditions and compression temperatures of approximately 700 K are different from the sequential auto-ignition caused by thermal stratifications. In the following, detailed chemical kinetic simulations are presented for the n-hexane cases illustrated in Figure 4 and Figure 6. The model assumes a perfectly homogeneous temperature of the compressed reactive mixture, which further allows making a clear differentiation between the two phenomena.

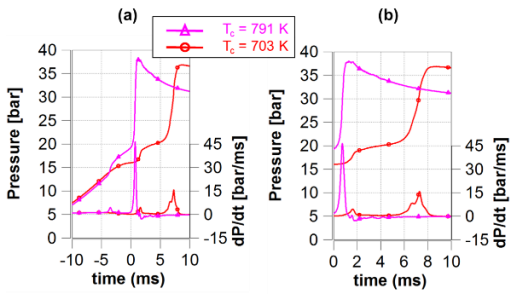

Figure 5. Pressure profiles demonstrating the multi-stage auto-ignition of n-hexane air mixture at 9.1 kg/m^3 density and different target temperatures: (a) overview of compression and auto-ignition, (b) zoom on the main ignition.

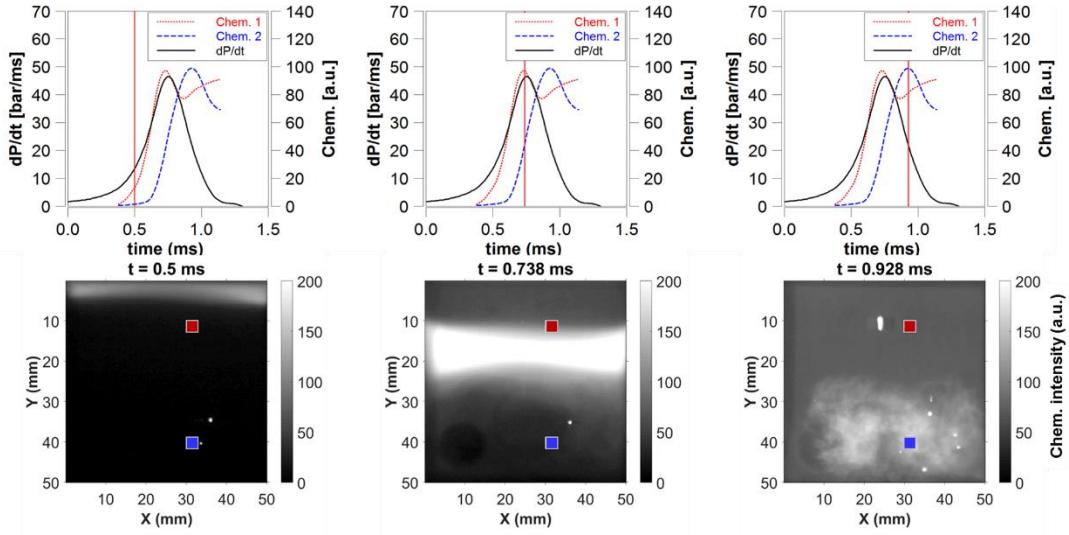

Figure 6. Illustration of the multi-stage auto-ignition of a lean diluted n-hexane mixture (T_c = 791 K).

3.2 *Experiments to simulation comparison*

The simulation results of n-hexane cases are presented in Figure 7 and Figure 8. These figures show the concentration profiles of the main species/radicals (CH2O, HO2, OH, and CO) that drive the various auto-ignition stages. The simulated concentrations of excited CH (CH*) and excited OH (OH*) are also reported together with simulated and experimental PRRs. Figure 7 demonstrates that the model predicts the experimentally observed three-stage PRR at 703 K with a small delay of approximately 2 ms compared to experiments. This is additional evidence that the observed phenomenon in experiments is chemically driven since the simulations do not account for any thermal stratification. The second and third peaks of the PRR are synchronized, respectively, with the peaks in the concentration of CH* and OH*. The maximum concentration of CH* is two orders of magnitude lower than that of OH*, which explains the weak chemiluminescence signal observed at the second stage in the cases of Figure 3 and Figure 4. During this main ignition split in two sub-stages, the concentration of CH2O, CO, and HO2 decreases progressively. The concentration of these radicals shows a sharper decrease in the higher

temperature case of Figure 8, where HTHR shows only one-stage of ignition. The moderate decrease in the CO and HO2 is governed by reactions highlighted in [1]. For the slow depletion of HO2, reaction HO2+OH=H2O+O2 has a large contribution to inhibit the reactivity across the high-temperature auto-ignition stages. Moving toward the latest auto-ignition stage, reaction CO+OH=CO2+H drives the fuel/air mixture to thermal runaway. Besides, the OH maximum concentration is an order of magnitude higher in the two-stage PRR case. The peak of OH radical is synchronized with the final stage in both cases. The chemistry behind the three-stage ignition is fully elaborated in [1].

The current detailed chemical kinetic simulations using a homogeneous batch reactor are consistent with the experimental results. Indeed, the three-stage PRR is a chemically driven phenomenon that is different from the sequential auto-ignition induced by thermal stratification. From the simulations, it is demonstrated that the maximum PRR of two-stage auto-ignition is four times higher than that of the three-stage case. On the other hand, the peak PRR of the simulation is twice higher than that of the experiment. This difference is most likely attributed to the sequential auto-ignition phenomenon that has been demonstrated in this flat piston RCM [21, 39].

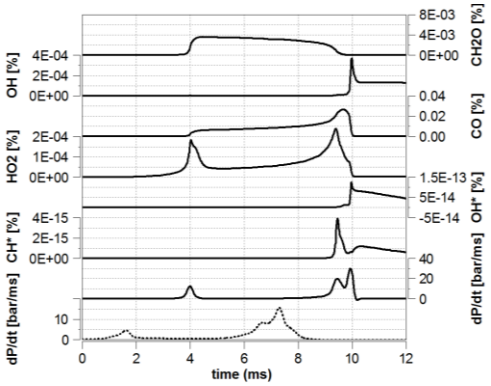

Figure 7. Overview of the main species profiles during the three-stage auto-ignition of n-hexane. The dashed line represents the experimental PRR. T_c = 703 K.

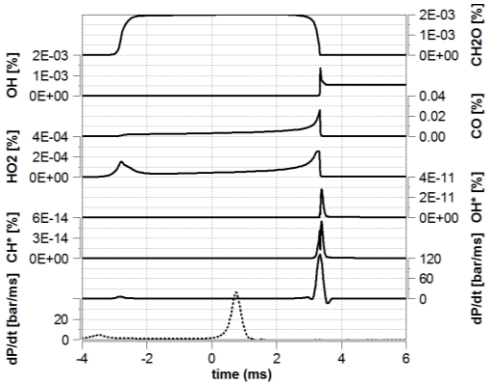

Figure 8. Overview of the main species profiles during the two-stage auto-ignition of n-hexane. The dashed line represents the experimental PRR. T_c = 791 K.

3.3 *Discussion*

So far, we did not see in the market any HCCI engine operating at high loads. This is likely explained by the lack of affordable technologies to control the reactivity and PRR of an HCCI mode. Nevertheless, several studies in the literature have demonstrated high load HCCI operation, achieved by optimized boosting and delayed phasing in [42] and by dual fuel and closed-loop control in [43]. Hence, the combustion phasing of HCCI may be controlled by different means: for instance by adjusting the boosting, the intake temperature, the dilution, or the compression ratio. However, the chemical kinetics and thermal stratification are the main parameters to control the PRR and it is difficult to decouple the effects of these two parameters.

In the present study, the temperature heterogeneity in the RCM is well characterized and the location of the adiabatically compressed gases is well-identified during the auto-ignition. The analysis of chemiluminescence in such configuration allowed us to make a clear interpretation of the PRR profile. Thus, we reported experimental evidence of a three-stage auto-ignition similar to the one observed in [1] and we demonstrated that this phenomenon is governed by chemical kinetics and is not caused by thermal stratification and sequential auto-ignition. This new finding cannot be demonstrated in engines, where the flow pattern, the temperature heterogeneity, and the test conditions are more complex to characterize. Our first results identify the three-stage ignition regime at temperatures below 750 K, which is lower than typical levels of HCCI engines. Such low compression temperature implies a lower compression ratio, which is not optimal for engine efficiency. This does not limit the current study as we focus on the understanding of a new auto-ignition behavior.

As a perspective, we suggest operating the engine at conditions where three-stage ignition chemistry would be predominant. If we can generate such a pattern of heat release, we would ease the control of the engine at HCCI mode. There is still a lot to understand about thermo-kinetic interactions and auto-ignition behavior that, from a fundamental point of view, is of benefit for IC engines, but also other propulsion concepts such as constant volume combustor, lean-premixed gas turbine engines, and MILD combustors.

4. Conclusion

This paper demonstrates evidence on three-stage auto-ignition with experiments performed in the flat piston RCM of PPRIME institute in Poitiers. The multi-stage ignition is observed when testing n-heptane and n-hexane at an equivalence ratio of 0.4 and a compression temperature near 700 K. The reactive mixtures feature a conventional two-stage auto-ignition when increasing the compression temperature to 791 K. Comparison of pressure profiles, PRR, and local chemiluminescence intensity demonstrates that the staged PRR is not correlated to sequential auto-ignition caused by thermal stratification inside the RCM chamber. The chemiluminescence

intensity, caused by the auto-ignition of the adiabatically compressed gases near 700 K, shows a small increase during the second stage and reaches its maximum at the third stage. This has been explained with detailed chemical kinetic simulations as these second and third stages are respectively synchronized with peaks in the concentrations of excited CH* and OH* radicals. The simulations show good agreement with experiments and predict the multi-stage feature with a minor delay. The three-stage auto-ignition reported in the current study is a chemically driven phenomenon, which is explained by reactions inhibiting thermal runaway in the HTHR regime. This work opens perspectives for trying to achieve three-stage ignition in engines to overcome limitations of HCCI operation by lowering the peak PRR.

Acknowledgment

The experimental work was supported by the French research agency (Association Nationale de la Recherche et de la Technologie ANRT), Renault S.A., and PPRIME Institute during the Ph.D. thesis of M. Ben Houidi (CIFRE N:384/2010). The simulation work was supported by King Abdullah University of Science and Technology (KAUST) Office of Sponsored Research (OSR) with funds given to the Clean Combustion Research Center. We acknowledge funding from the KAUST Clean Fuels Consortium and its member companies.

References

[1] S.M. Sarathy, E.-A. Tingas, E.F. Nasir, A. Detogni, Z. Wang, A. Farooq, H. Im, Three-stage heat release in n-heptane auto-ignition, Proceedings of the Combustion Institute 37 (2019) 485-492.
[2] F. Zhao, T.N. Asmus, D.N. Assanis, J.E. Dec, J.A. Eng, P.M. Najt, Homogeneous charge compression ignition (HCCI) engines, SAE Technical Paper, 2003.
[3] M. Christensen, B. Johansson, P. Amnéus, F. Mauss, Supercharged homogeneous charge compression ignition, SAE transactions, (1998) 1129-1144.
[4] S. Gan, H.K. Ng, K.M. Pang, Homogeneous charge compression ignition (HCCI) combustion: implementation and effects on pollutants in direct injection diesel engines, Applied energy 88 (2011) 559-567.
[5] S. Tanaka, F. Ayala, J.C. Keck, J.B. Heywood, Two-stage ignition in HCCI combustion and HCCI control by fuels and additives, Combustion and flame 132 (2003) 219-239.
[6] M. Christensen, A. Hultqvist, B. Johansson, Demonstrating the multi fuel capability of a homogeneous charge compression ignition engine with variable compression ratio, SAE transactions, (1999) 2099-2113.
[7] S. Saxena, I.D. Bedoya, Fundamental phenomena affecting low temperature combustion and HCCI engines, high load limits and strategies for extending these limits, Progress in Energy and Combustion Science 39 (2013) 457-488.
[8] R.D. Reitz, G. Duraisamy, Review of high efficiency and clean reactivity controlled compression ignition (RCCI) combustion in internal combustion engines, Progress in Energy and Combustion Science 46 (2015) 12-71.
[9] M. Richter, J. Engström, A. Franke, M. Aldén, A. Hultqvist, B. Johansson, The influence of charge inhomogeneity on the HCCI combustion process, Report No. 0148-7191, SAE Technical Paper, 2000.
[10] S.M. Aceves, D.L. Flowers, C.K. Westbrook, J.R. Smith, W. Pitz, R. Dibble, M. Christensen, B. Johansson, A multi-zone model for prediction of HCCI combustion and emissions, SAE transactions, (2000) 431-441.
[11] J. Griffiths, P. Halford-Maw, D. Rose, Fundamental features of hydrocarbon autoignition in a rapid compression machine, Combustion and flame 95 (1993) 291-306.
[12] E.-A. Tingas, Z. Wang, S.M. Sarathy, H.G. Im, D.A. Goussis, Chemical kinetic insights into the ignition dynamics of n-hexane, Combustion and Flame 188 (2018) 28-40.
[13] J.P. Szybist, D.A. Splitter, Pressure and temperature effects on fuels with varying octane sensitivity at high load in SI engines, Combustion and Flame 177 (2017) 49-66.
[14] W. Hwang, J. Dec, M. Sjöberg, Spectroscopic and chemical-kinetic analysis of the phases of HCCI autoignition and combustion for single-and two-stage ignition fuels, Combustion and Flame 154 (2008) 387-409.

[15] D. Vuilleumier, D. Kozarac, M. Mehl, S. Saxena, W.J. Pitz, R.W. Dibble, J.-Y. Chen, S.M. Sarathy, Intermediate temperature heat release in an HCCI engine fueled by ethanol/n-heptane mixtures: An experimental and modeling study, Combustion and flame 161 (2014) 680-695.
[16] G. Shibata, T. Urushihara, Dual phase high temperature heat release combustion, SAE International Journal of Engines 1 (2009) 1-12.
[17] G. Shibata, T. Urushihara, Realization of dual phase high temperature heat release combustion of base gasoline blends from oil refineries and a study of HCCI combustion processes, SAE International Journal of Engines 2 (2009) 145-163.
[18] J.E. Dec, W. Hwang, M. Sjöberg, An investigation of thermal stratification in HCCI engines using chemiluminescence imaging, SAE Transactions, (2006) 759-776.
[19] C. Strozzi, J. Sotton, A. Mura, M. Bellenoue, Characterization of a two-dimensional temperature field within a rapid compression machine using a toluene planar laser-induced fluorescence imaging technique, Measurement Science and Technology 20 (2009) 125403.
[20] M. Ben-Houidi, J. Sotton, A. Claverie, C. Strozzi, M. Bellenoue. Application of high-speed PIV and Toluene PLIF techniques to study aerodynamics and thermal stratification inside a flat piston Rapid Compression Machine. In: editor^editors. 18th International Symposium on the Application of Laser and Imaging Techniques to Fluid Mechanics; 2016. p.
[21] M.B. Houidi, J. Sotton, M. Bellenoue, Interpretation of auto-ignition delays from RCM in the presence of temperature heterogeneities: Impact on combustion regimes and negative temperature coefficient behavior, Fuel 186 (2016) 476-495.
[22] C.-J. Sung, H.J. Curran, Using rapid compression machines for chemical kinetics studies, Progress in Energy and Combustion Science 44 (2014) 1-18.
[23] S.S. Goldsborough, S. Hochgreb, G. Vanhove, M.S. Wooldridge, H.J. Curran, C.-J. Sung, Advances in rapid compression machine studies of low-and intermediate-temperature autoignition phenomena, Progress in Energy and Combustion Science 63 (2017) 1-78.
[24] D. Bradley, M. Lawes, M. Materego. Interpretation of auto-ignition delay times measured in different rapid compression machines. In: editor^editors. 25th International Colloquium on the Dynamics of Explosions and Reactive systems; 2015: Leeds. p.
[25] G. Mittal, M. Chomier, Interpretation of experimental data from rapid compression machines without creviced pistons, Combustion and Flame 161 (2014) 75-83.
[26] S. Goldsborough, G. Mittal, C. Banyon, Methodology to account for multi-stage ignition phenomena during simulations of RCM experiments, Proceedings of the Combustion Institute 34 (2013) 685-693.
[27] N. Bourgeois, H. Jeanmart, G. Winckelmans, O. Lamberts, F. Contino, How to ensure the interpretability of experimental data in Rapid Compression Machines? A method to validate piston crevice designs, Combustion and flame 198 (2018) 393-411.
[28] S. Yousefian, F.o. Gauthier, A. Morán-Guerrero, R.R. Richardson, H.J. Curran, N.J. Quinlan, R.F. Monaghan, Simplified approach to the prediction and analysis of temperature inhomogeneity in rapid compression machines, Energy & Fuels 29 (2015) 8216-8225.
[29] G. Mittal, M.P. Raju, C.-J. Sung, Vortex formation in a rapid compression machine: Influence of physical and operating parameters, Fuel 94 (2012) 409-417.
[30] G. Mittal, M. Chomier, Effect of crevice mass transfer in a rapid compression machine, Combustion and flame 161 (2014) 398-404.
[31] G. Mittal, S. Gupta, Computational assessment of an approach for implementing crevice containment in rapid compression machines, Fuel 102 (2012) 536-544.
[32] G. Mittal, A. Bhari, A rapid compression machine with crevice containment, Combustion and flame 160 (2013) 2975-2981.
[33] N. Bourgeois, S.S. Goldsborough, H. Jeanmart, F. Contino, CFD simulations of Rapid Compression Machines using detailed chemistry: Evaluation of the 'crevice containment'concept, Combustion and flame 189 (2018) 225-239.
[34] C. Strozzi, J. Sotton, A. Mura, M. Bellenoue, Experimental and numerical study of the influence of temperature heterogeneities on self-ignition process of methane-air mixtures in a rapid compression machine, Combustion Science and Technology 180 (2008) 1829-1857.
[35] E. Monteiro, J. Sotton, M. Bellenoue, N.A. Moreira, S. Malheiro, Experimental study of syngas combustion at engine-like conditions in a rapid compression machine, Experimental Thermal and Fluid Science 35 (2011) 1473-1479.
[36] C. Strozzi, A. Mura, J. Sotton, M. Bellenoue, Experimental analysis of propagation regimes during the autoignition of a fully premixed methane–air mixture in the presence of temperature inhomogeneities, Combustion and Flame 159 (2012) 3323-3341.
[37] S.S. Goldsborough, Evaluating the heat losses from HCCI combustion within a rapid compression expansion machine, Report No. 0148-7191, SAE Technical Paper, 2006.

[38] S.S. Goldsborough, C. Banyon, G. Mittal, A computationally efficient, physics-based model for simulating heat loss during compression and the delay period in RCM experiments, Combustion and Flame 159 (2012) 3476-3492.
[39] M.B. Houidi, J. Sotton, M. Bellenoue, C. Strozzi, Effects of low temperature heat release on the aerodynamics of a flat piston rapid compression machine: Impact on velocity and temperature fields, Proceedings of the Combustion Institute 37 (2019) 4777-4785.
[40] K. Zhang, C. Banyon, J. Bugler, H.J. Curran, A. Rodriguez, O. Herbinet, F. Battin-Leclerc, C. B'Chir, K.A. Heufer, An updated experimental and kinetic modeling study of n-heptane oxidation, Combustion and Flame 172 (2016) 116-135.
[41] Y.B. Zeldovich, Regime classification of an exothermic reaction with nonuniform initial conditions, Combustion and Flame 39 (1980) 211-214.
[42] J.E. Dec, Y. Yang, Boosted HCCI for high power without engine knock and with ultra-low NOx emissions-using conventional gasoline, SAE International Journal of Engines 3 (2010) 750-767.
[43] J.-O. Olsson, P. Tunestål, G. Haraldsson, B. Johansson, A turbo charged dual fuel HCCI engine, Report No. 0148-7191, SAE technical paper, 2001.